Implementation of Tracking Algorithm for Mesoscale Convective Systems in Flood Disaster Events Over East Belitung, Indonesia

Sanaullah Zehri[1]*, Agung Adiputra[1], Hasna Rofifah[2], Afiq Mahasin[3]

[1]Departemen of Geography Education, Universitas Muhammadiyah Prof. Dr. Hamka, Ciracas, Jakarta, 13830

[2]Marine and Science Technology, IPB University, Dramaga, Bogor, 16680

[3]Oceanography, Diponegoro University, Semarang, 50275

*E-mail: sanaullah@uhamka.ac.id

ABSTRACT

Flooding is a significant problem with a high probability of affecting both people and infrastructure. Predicting floods is difficult because of its association with a quickly evolving convective system. Furthermore, simulating the dynamics of mesoscale convective systems (MCSs) is essential for enhancing our comprehension of the heavy precipitation systems that induce flooding. A flood in east Belitung on July 15, 2017, was suspected to have been caused by convective activity. The flood was preceded by persistent heavy rainfall from July 14 – 16, 2017, with the peak rainfall accumulation reaching >180 mm hr^{-1} on July 15, 18:00 UTC. This research aims to identify the type of storm system formed over the study area associated with heavy rainfall, simulate the propagation of MCSs, and increase the utilization of the algorithm detecting storms in Indonesia. We implemented the Tracking Algorithm for Mesoscale Convective Systems (TAMS) algorithm. TAMS allows for identifying, tracking, classifying, and variable-assigning to MCSs. TAMS integrates area-overlapping and projected-cloud-edge tracking approaches to enhance the likelihood of capturing the progression of the systems through time. We assigned the precipitation data from Global Satellite Mapping of Precipitation (GSMaP) to calculate corresponding statistics within the cloud area. We reveal that two cases of Convective Cloud Clusters (CCCs) were responsible for the persistent heavy rainfall. The 1st case occurred on July 14, 12:00 (initial) – July 15, 13:00 (dissipating) UTC, with an average eccentricity (ε) = 0.85 and initially formed around west Kalimantan propagated until southwest Sumatra. The 2nd case occurred on July 15, 14:00 – July 16, 08:00 UTC, average ε = 0.74, and initially formed at west Kalimantan and propagated until southwest Belitung. The pair of CCCs was triggered by a meso-low pressure and moist-warm air, which may have helped extend the lifetime of the CCCs. The elevated sea surface temperature (SST) around Belitung and northwest Kalimantan induces convective activity and forms clouds.

Keywords: tracking, mesoscale convective system, mesoscale convective complexes, east Belitung, heavy rainfall

1. Introduction

Indonesia lies in a tropical area, its also influenced by monsoonal activity and Inter-tropical Convergence Zone (ITCZ), is exposed to heavy rain accumulation. Indonesia also has thousands of islands, leading to various climatic phenomena such as landslides and floods [1]–[5]. Flood events are typically disasters that occur in Indonesia. Hydrometeorological disasters can affect an area, causing damage to infrastructure and loss of life. In Indonesia, the incidence of flood disasters has increased yearly [6]. Floods can be caused by various factors, including heavy rainfall intensity, population increase, deforestation, the destruction of watershed storage, river channel development planning errors, river siltation, and major shifts in land use, which have led to the reduction of retention areas, which, along with climate change, render the country particularly susceptible to flooding [7]. On July 14 – 16, 2017, a heavy rainfall event occurred in Bangka Belitung province, and this persistent rain caused flooding in the region. Based on Global Satellite Mapping of Precipitation (GSMaP) data, the three-hour accumulation value shows a peak rainfall >180 mm hr-1 depicted in Figure 2. The Lalang-Manggar station recorded 653 mm day-1 of rainfall with a duration of rainfall ± 20 hours. This data is the highest value recorded across every Belitung station, with other Indonesian Agency for Meteorology, Climatology, and Geophysics (BMKG) stations reporting an upsurge in rain accumulation on July 15 [8]. In the previous research, the presence of land depressions was due to mining excavations around the watershed and catchment area. Consequently, it disrupted the water discharge volume and caused water to overflow [9], [10]. Rega stated in its research that the government has already mitigated the problem by implementing a drainage program. However, various obstacles, such as rubbish, vegetation, and sedimentation, caused the drainage not to work properly in lowering the danger of flood disaster. These challenges can arise due to funding limits and a lack of community participation [11]. Heavy rainfall events are associated with mesoscale convection activity, broadly referred to as Mesoscale

IMPLEMENTATION OF TRACKING ALGORITHM..Sanaullah Zehri, et al.

69

Convective Systems (MCSs) [12], [13]. MCSs are complex, organized thunderstorms that may persist for hours. To see how MCSs formed, the clouds develop as a reaction to convective instability. Integrate and organize upscale into a single cloud system with a massive upper cirriform cloud structure and rainfall covering enormous contiguous rain domains [14]. Cloud clusters contribute to a substantial quantity of precipitation worldwide, frequently resulting in catastrophic precipitation events that severely threaten life and livelihood [15]. MCSs frequently create severe weather with significant rainfall. Evans and Jaskiewicz found that MCSs lasting longer than 6 hours can produce 50% of total precipitation in the region [16]. Nuryanto et al. said that the development of MCSs over the Greater Jakarta (GJ) produced heavy rainfall on January 15 – 18, 2013 [17]. Yulihastin et al. studied the defined type of MCSs, Mesoscale Convective Complexes (MCCs), and found that the growth of MCCs controlled heavy rainfall, as well as that long-lived MCCs, were sustained by a back-building mechanism. It leads to a severe flash flood on July 13, 2020 [18]. On the date of the heavy rainfall leading to flood events in east Belitung, we monitored the cloud-top temperature data from Himawari 8. A large cloud cluster was observed over the region at that time. At first, we assumed the convective system was classified as MCCs. Then, it motivates us to analyze the properties of the cloud systems to answer that assumption.

Conducting analysis related to convective activity could be challenging, especially when certain algorithms are needed to detect cloud clusters and ultimately determine the type of convective systems. The "Grab'em Tag'em, Graph'em" (GTG) detects cloud clusters utilizing infrared data and a connected graph node for tracking through the area overlap approach [19]. This algorithm is a Python-based tracker and could be utilized for satellite data. For instance, Putri et al. studied the properties of MCSs in Indonesia using the GTG algorithm with input data from Multi-functional Transport Satellite-1R, whose one of the results could distinguish cloud microphysical properties of MCSs at sea and land [20]. Nuryanto applied the GTG algorithm to identify occurrences of heavy rainfall in Jakarta, successfully detecting a convective cloud structure with a cold core area of cloud shield associated with heavy rainfall [21]. The "Tracking Algorithm for Mesoscale Convective Systems" (TAMS) algorithm is used to locate, track, classify, and measure any variable desired throughout the life cycle of MCSs [22]. This automatic computerized tracking algorithm combines the area-overlapping and modified projection-cloud-edge approaches. Using satellite-derived datasets, TAMS was initially served to develop and evaluate MCSs across Africa and their association with African Easterly Waves (AEW) [23]. Considering the

advantages of the TAMS algorithm for tracking and adding variables desired to enhance the analysis, we applied it to track and characterize the properties of convective clouds over the region. Our research aims to identify the type of storm system formed in the study area associated with heavy rain, simulate the propagation of MCSs around eastern Belitung, and increase the utilization of the algorithm in detecting storms in Indonesia. The GTG algorithm is widely used by researchers to detect storm systems. Therefore, the initial use of a new algorithm, i.e., TAMS, in Indonesia will inspire researchers to try, improve, and compare the available algorithms and produce the best results in detecting and classifying cloud systems for early warning systems in heavy and extreme rainfall events.

2. Methods

We applied TAMS v2.0 to get an advance for assigning any variable data to the algorithm with the following four-step stages: 1) Identify, 2) Tracking, 3) Classify, and 4) Assigning variables. Compared to TAMS v2.0, TAMS v1.0 is limited to assigning variable data (which is only considered for precipitation data). The documentation of the applied TAMS algorithm can be accessed through this website:(https://tams.readthedocs.io/en/latest/index.html), which provides instructions for Python (pip-installation methods) and an example of running extended and independently. For preparation data as an input for TAMS, we prepared the black body temperature (TBB) data from Himawari-8 provided by the database-rish Kyoto (https://database.rish.kyoto-u.ac.jp/). The variable for TBB data had an 11 μm spectral band, one hourly time resolution, and a horizontal resolution of 0.1 x 0.1 degree [24]. This cloud-top temperature data is preserved for the stages of Identifying, Tracking, and Classifying the properties of cloud systems. Other variables for consideration to be assigned are precipitation data from Global Satellite Mapping of Precipitation (GSMaP) with one hourly time resolution and a horizontal resolution of 0.1 x 0.1 degree [25]. Both data cover a domain area in Figure 1 and time spanning from July 14 – 16, 2017. The workflow of the TAMS algorithm can be seen in Figure 2.
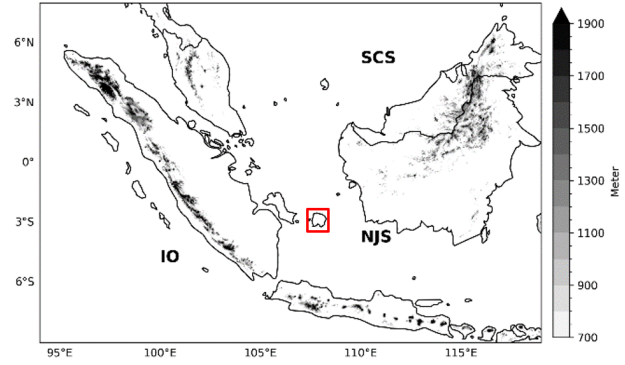
In the identification stage, the algorithm detects the cloud areas, i.e., cloud elements (CEs). Our configuration is set as the minimum <219 K for deep convective and <235 K for the maximum value linked to the convective activity [26]–[28]. The 235 K areas contain an embedded cold core (219 K) as a contour with areas of ≥ 4000 km^2 [29]. Therefore, 235 K areas become TAMS CEs, which are candidates for the next two stages: tracking and classification. In the tracking stage, each current detected CE will be linked to other previous CEs to track MCSs. A single

CE time, i.e., CE$_{time(t_i)}$, has only one parent at t_{i-1}; it could get split when multiple CEs have the same parent. All the connected CEs provide an (id) of MCS that will be important for tracking. Its also essential that there is more than one (id) at a given time. In the classifying stage, all the CEs that contain area, shape, and time can be classified into MCS of the criteria given by the initial previous TAMS algorithm research in Table 1. TAMS defined four classifications of MCS: Mesoscale Convective Complexes (MCCs), Convective Cloud Clusters (CCCs), Disorganized Long-Lived (DLLs), and Disorganized Short-Lived (DSLs). Those four classes are based on two main categories: organized and disorganized systems. Only the MCCs have a shape criterion with an eccentricity (ε) < 0.7. This eccentricity calculation was fitted to the CE, with CE having an eccentricity close to 0, corresponding to a circle. On the other hand, the CCCs sometimes get more elongated shapes that fail to be classified as MCCs while the area meets the criteria and vice versa. The short duration of CE that is not sustained for ≥6 hours is classified as a disorganized system, which is DLS and DLL. We assign the rainfall data from GSMaP to diagnose the convective activity over the region of CE. In previous research, it was said that to get a good match, distinct clouds, and any variable, at least users' data include the same resolution of grid and time, but the function is not limited to different resolution data. After assigning the data, we can see that a match propagation between precipitation in the cold core extracted to mean precipitation over CE with eccentricity and area of MCSs in the next section.
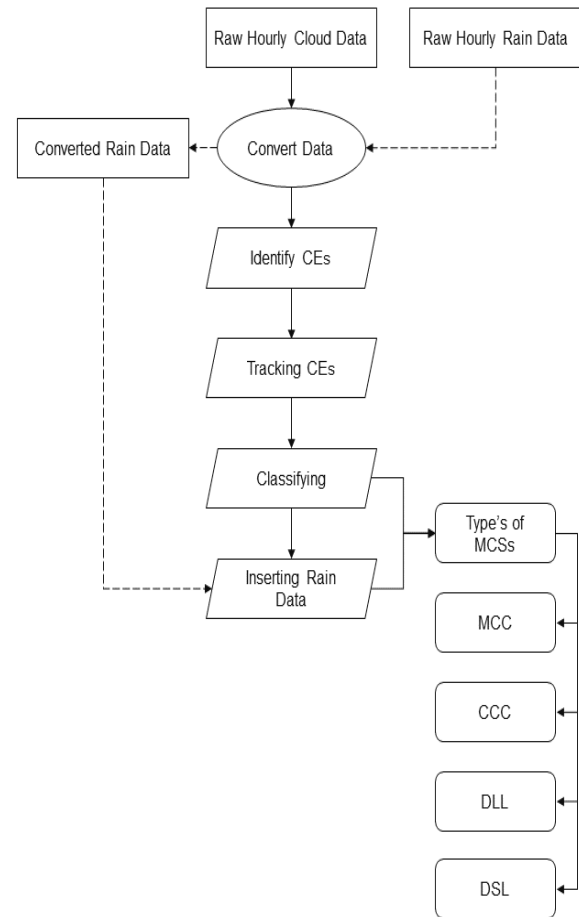
To further investigate the heavy rainfall event, we analyze the air-sea interaction with the spatial results of high-resolution sea surface temperature (SST) data obtained from Operational Sea Surface Temperature and Ice Analysis (OSTIA) [30]. Meso-level pressure can be analyzed by the movement of winds; we used high-resolution wind data from Cross-Calibrated Multi-Platform (CCMP) [31]. We also investigate the moisture transport to see the moist area with the following equation:

$$IVT = \left[\left(\frac{1}{g} \int_b^a qu\, dp \right)^2 + \left(\frac{1}{g} \int_b^a qv\, dp \right)^2 \right]^{1/2} \quad (1)$$

where g is gravitational acceleration, a is set for maximal from each layer; 300mb, b is the minimum from each layer; 1000mb, q for specific humidity (g/kg), p for pressure (Pa), u and v for zonal and meridional wind. Data can be accessed from ERA 5 Reanalysis [32].

Figure 1. Research domain area (90° - 120°E, 7°N - 7°S), shaded information: elevation (meter), and (107.3° - 108.4°E, 2.45° - 3.35°S, red box) for mean area domain initiated for graphical plot on Figure 3, SCS, IO, NJS for South China Sea, Indian Ocean, North Java Sea, respectively.

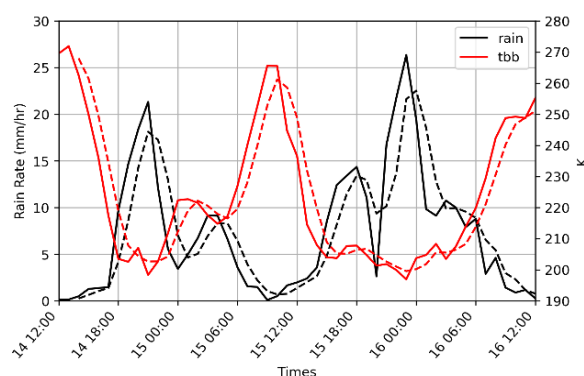**Figure 2.** Workflow of TAMS for detecting MCSs in this study.

IMPLEMENTATION OF TRACKING ALGORITHM,...Sanaullah Zehri, et al.

71

Table 1. Criteria for MCSs used in TAMS following the previous research

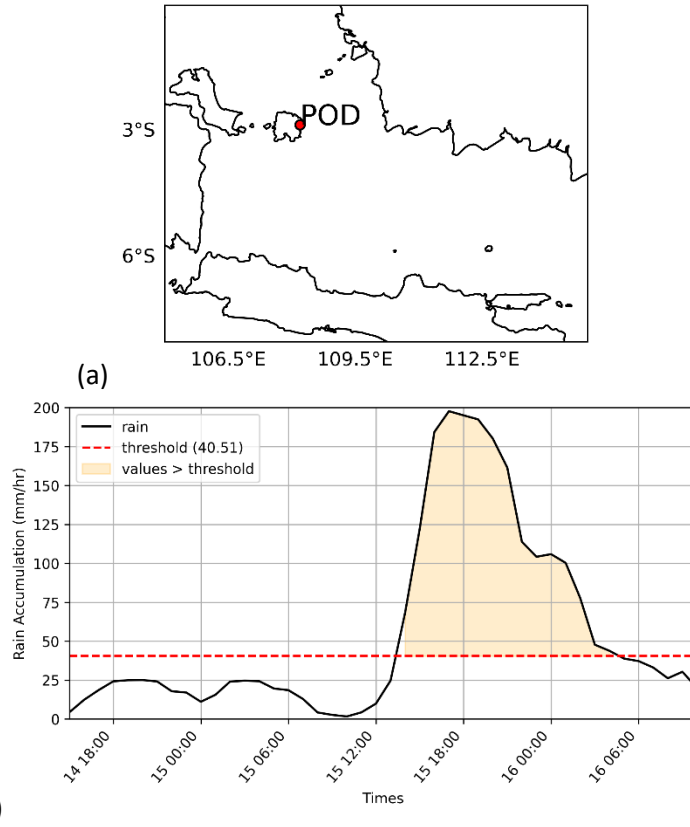| Organized systems	Disorganized systems
Mesoscale convective complex (MCC)	Disorganized long-lived (DLL)
Size: <219 K region has an area ≥25.000 km2 *(i)* <235 K region has an area ≥50.000 km^2 *(ii)*. Duration: size definitions are met for ≥6h. Shape: ε $= \sqrt{1 - \left(\frac{b^2}{a^2}\right)}$ ≥0.7	Temperature: <219 K. Duration: sustains for ≥6 h. No size or shape criteria
Convective cloud cluster (CCC)	Disorganized short-lived (DSL)
Size: <219 K region has area ≥25.000 km^2. Duration: size definitions are met for ≥6 h. Shape: no shape criteria	Temperature: <219 K. Duration: sustains for ≤3h. No size or shape criteria

3. Result and Discussion

Heavy Rainfall and Background Conditions.
Heavy rainfall occurred in east Belitung from July 14 – 16, 2017. This event seems unusual because the average rainfall value on the other days was stable, considering the regional-scale activity of the Australian monsoon movement. However, the east Belitung area has an equatorial rainfall type. The equatorial rainfall pattern is characterized by two peaks in the rainy seasons in March and October [33], and the storms that cause heavy rainfall should not form unless there are additional contributing factors. We calculate the mean precipitation over the red box area in Figure 1 to see the temporal characteristics of precipitation compared to the TBB data, as shown in Figure 3.
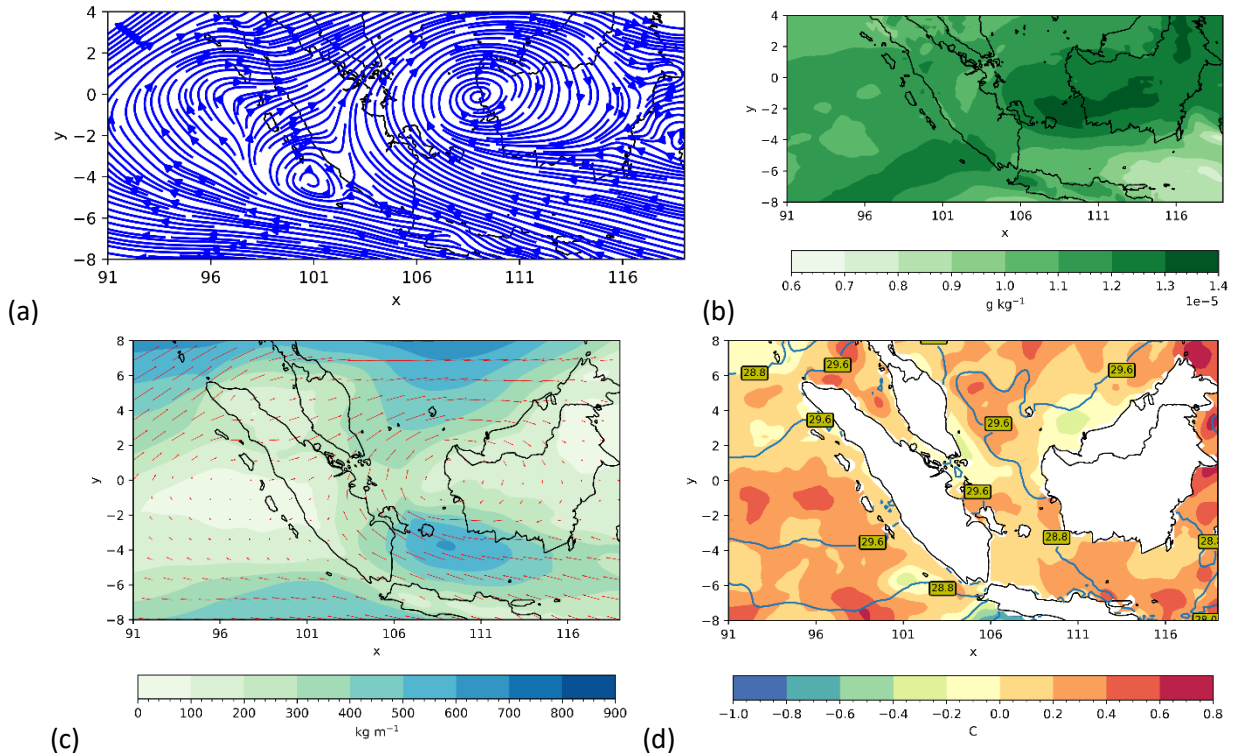

Figure 3. y-axis left (mm hr^{-1}) for three hourly rain rates (black solid band), and y-axis right for black body temperature (kelvin) with same temporal ratio (red solid line). Then, smoothing data for rain rate (black dashed line) and black body temperature (red dashed line) with three hourly average moving windows from July 14, 12:00 – July 16, 12:00 UTC.

Based on the Figure 3, rainfall activity starts at around July 14, 17:00, reaching the first peak around 20:00 at a rate of 23 mm hr^{-1}. The second peak occurred on July 15, 18:00, with a rate of 14 mm hr^{-1}, and for the next 6 hours at July 16, 00:00, the rain rate reached the highest of all the peaks, around 26 mm hr^{-1}. Some rainfall occurs in the early morning, which may associated with the land-sea breeze mechanism [2], [34]. It also can be seen that the TBB data has a value <219 K associated with deep convective on each peak rainfall. It represents symmetrical values; while the TBB data fell, the rain rate would increase. Yulhastin et al. found that early morning precipitation (EMP) distribution is not bound to the movement of land and sea breeze phases, resulting in less predictable precipitation episodes [35]. EMP is typically related to South China Sea Cold Tongue (SCS-CT) and Cross Equatorial Notherly Surge (CENS) activity in particular months, such as January and February [36], [37]. Then, the occurrence of heavy rainfall in Belitung does not match any of the previously described factors. Therefore, other factors can influence this event. We evaluate this heavy rainfall by calculating percentile-95 (p95) through the rain data set and getting the threshold value, which is 40.51 mm. In this case, the heavy rainfall became extreme starting on July 15, 12:00, based on the p95 value, and reached peaks at 17:00, around 197 – 200 mm. The coordinates of the point of disaster (POD) were obtained from the National Disaster Management Agency's Disaster Information Indonesia (DIBI) website (https://dibi.bnpb.go.id/). POD represents the precise location where the flood disaster occurred. This confirms the previous discussion that the precipitation event occurred on the July 14, before the flood disaster. The results of our analysis demonstrate the presence of mesoscale activity that can influence the active convective dynamics in the west, thereby engaging air-sea interactions, which are also associated with the modulation of the convective system illustrated in

(a)

(b)

Figure 4. (a). Point of disaster (108.2°E, 2.85°S). (b). six hourly rain accumulation from the point of disaster (black solid line), the threshold extreme (red dashed line) for percentile-95 (p95) value: 40.51 mm, and an area orange fill was values > threshold.

(a)

(b)

(c)

(d)

Figure 5. (a). Spatial map of wind at 850 mb (streamlines) averaged from July 14 – 16, 2017. (b). same as (a) but for specific humidity. (c). same as (a), but for vertically integrated vapor transport from 1000 to 300 mb overlaid with wind (red vector) at 850mb. (d). same as (a), but for sea surface temperature anomaly (shaded), and normal condition (contour line).

IMPLEMENTATION OF TRACKING ALGORITHM...Sanaullah Zehri, et al.

73

Figure 5. Meso-low pressure with anti-cyclonic circulation occurs over the western part of Kalimantan, as shown in Figure 5(a). This movement circulation is defined as anti-cyclone (clockwise) due to this circulation lies in the part of the northern hemisphere. During the Asian monsoon, a phenomenon in the form of counterclockwise (cyclone) rotation circulation is observed. This vortex is located in the northwest region of the island of Kalimantan and is frequently associated with heavy rainfall and flood disasters.

The interaction of Asian monsoon winds with winds from the southeast in the northwest region of Kalimantan results in the formation of a vortex [38]. This circulation called as Borneo Vortex (BV). In this case, this circulation couldn't be defined as BV because it does not meet BV's standard time occurrences and wind movement patterns [39]. This circulation makes the air around it more humid and transports the moist airflow from the eastern part of the North Java Sea (NJS) to Belitung and the eastern part of Kalimantan. It is also possibly influenced by the Australian monsoon that contributes to bringing air from the eastern part of Indonesia. Cyclonic circulation and humid patterns also occurred around the southwest part of Sumatra on July 14 – 16, 2017.

Additionally, the warming of sea surface temperature around Karimata strait (KS), valued at around >29°C, and the shifting temperature that becomes warmer will be the perfect conditions to produce convective activity. Tan et al. said the if the wind advection is weakened, i.e. the wind cannot carry away the latent heat released by the oceans, then sea surface temperatures will be increased [40].

During the dry season, the monsoon breezes move from Australia to Asia, and the advection of wind around the South China Sea (SCS) and Karimata Strait (KS) weakens, which is latent heat that escapes from SCS and KS into the atmosphere, raising the sea surface temperature. The warm SST influences some occurrences of convective activity; this warm SST can be a fuel of the updraft and tends to make the cloud systems live longer. Previous research by Yulihastin et al. reveals that Seroja cyclogenesis could be formed in Indonesia due to heat traps in the Maluku Sea [41]. On the topography, Previous research examined the river watersheds in east Belitung. It's said that the Manggar, Linggang, and Sago watersheds are all located near the flooding area. Table 2 indicates that river silting occurs across the watersheds despite considering that the landscape is generally flat. The sandy soil type in each watershed inhibits infiltration from runoff. Then, it

was discovered that the watershed's land use was dominated by mining, plantation, and illegal logging. The Forest Area Supervisory Agency (BPKH) statistics analysis reveals a significant rise in land cover between 2015 and 2016. The plantation area increased to >40000 hectares in 2015 and continues to grow through 2016. In 2015 and 2016, there also was a reduction in secondary dryland forests with an area of <5000 hectares [42]. This will end up increasing the conveyance coefficient and flood flow discharge. Therefore, with land conversion activities and the problems described, persistent and extreme rainfall events will lead to flooding disasters, and this disaster will return if there is no good resolution.

TAMS Algorithm. We implemented the TAMS algorithm from July 14, 00:00 – July 16, 23:00. TAMS automatically provides results from each convective system of CEs detected at each time. CEs are then classified into MCS types. CCCs are the type of MCS that contributes to flooding in eastern Belitung, as shown in Table 3. We filtered the raw results from TAMS, showing that CCC formed and tracked around east Belitung twice. Overall, the TAMS algorithm results in an area which we refer to in this study as the "boundary area," representing the outer boundary of the MCS type. The boundary area contains temperature data that has been set prior to the execution of the algorithm and comprises a cold core area of cloud associated with heavy precipitation.

In figures 6 and figure 7, We tested the boundary area of CCC properties generated by TAMS and compared them to rainfall data from GSMaP. We have provided a visual representation of the outer boundary, covering the eastern part of the Belitung area. The first initiation was detected at 12:00, covering an area around 470022 km^2. For the next two hours at 19:00, the CCC experience split into two parts. As stated in the previous section, multiple CEs are detected simultaneously in the same parents and system. The change would occur by CEs splitting away from the first system but still classified in the previous parents. Therefore, both CCCs continue to propagate the system and dissipate for the south CCC at July 15, 13:00. The same conditions were observed at 15:00 when an enormous CCC was split into two parts.
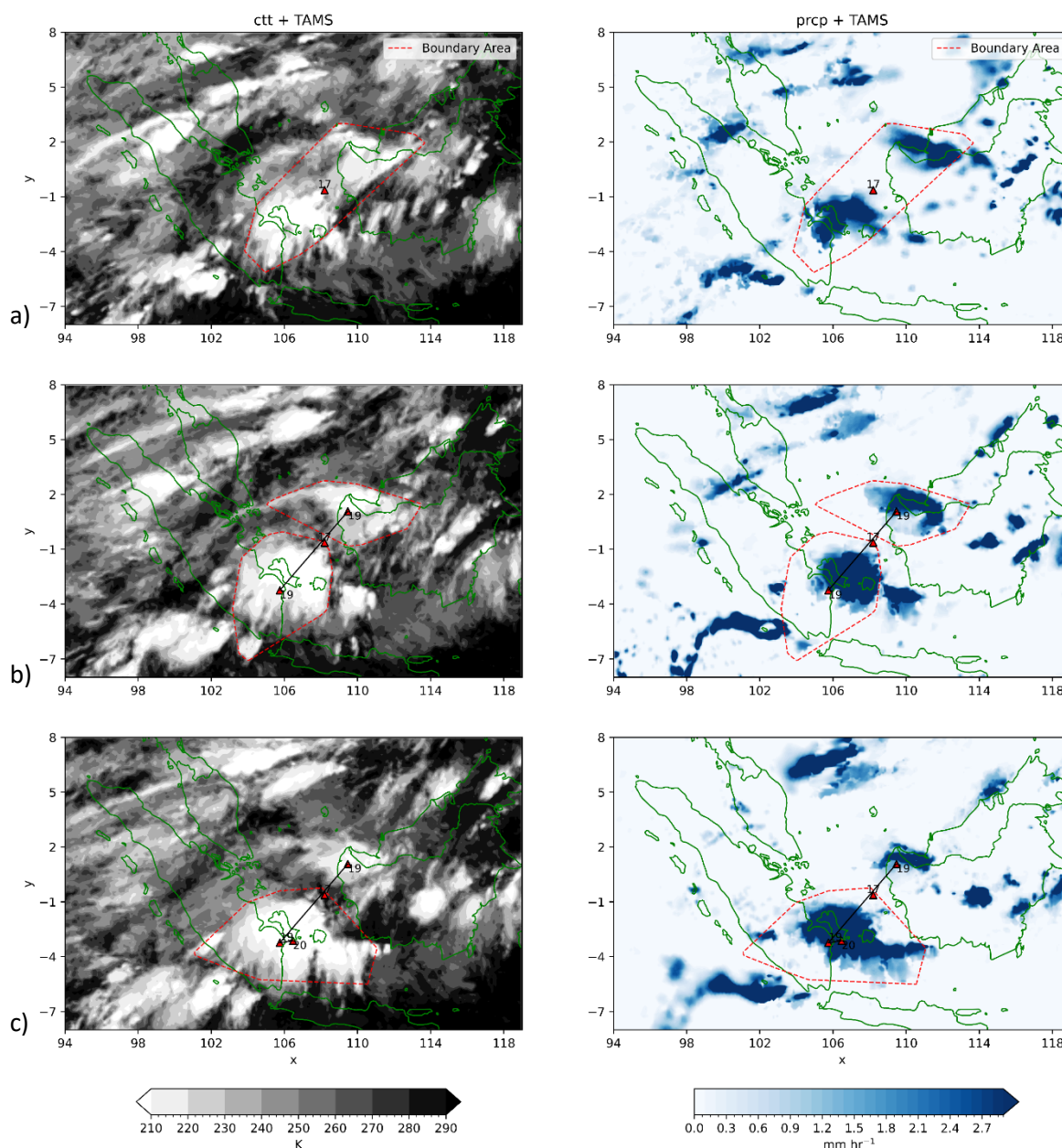
Table 2. Watersheds description by Sabri et al., 2017

Watersheds	Level	Type of soil
Manggar	Shallow	Sandy
Linggang	Shallow	Sandy
SAGU	Shallow	Sandy

Table 3. The filtered result from the TAMS algorithm

Time (UTC)	Stage	Cases	x	y	Area (km^2)	Eccentricity
14 July, 12:00	Initiation	First case	106.59	-0.78	470022	0.87
15 July, 13:00	Dissipation		99.82	-5.54	342272	0.91
15 July, 14:00	Initiation	Second	110.29	1.29	637651	0.93
16 July, 08:00	Dissipation	case	106.39	-4.26	151539	0.56

Figure 6. (a). cloud-top temperature (TBB) (contour) overlaid with a boundary of CE from TAMS (red dashed line) for a first case at first initiation July 14, 17:00 (left) and prcp: precipitation (mm hr-1) overlaid with a boundary of CE from TAMS (red dashed line) for a first case at first initiation July 14, 17:00 (right). (b). same as (a), but for 19:00 (left) and (right). (c). same as (a) but for 20:00 (left) and (right)

IMPLEMENTATION OF TRACKING ALGORITHM...Sanaullah Zehri, et al.
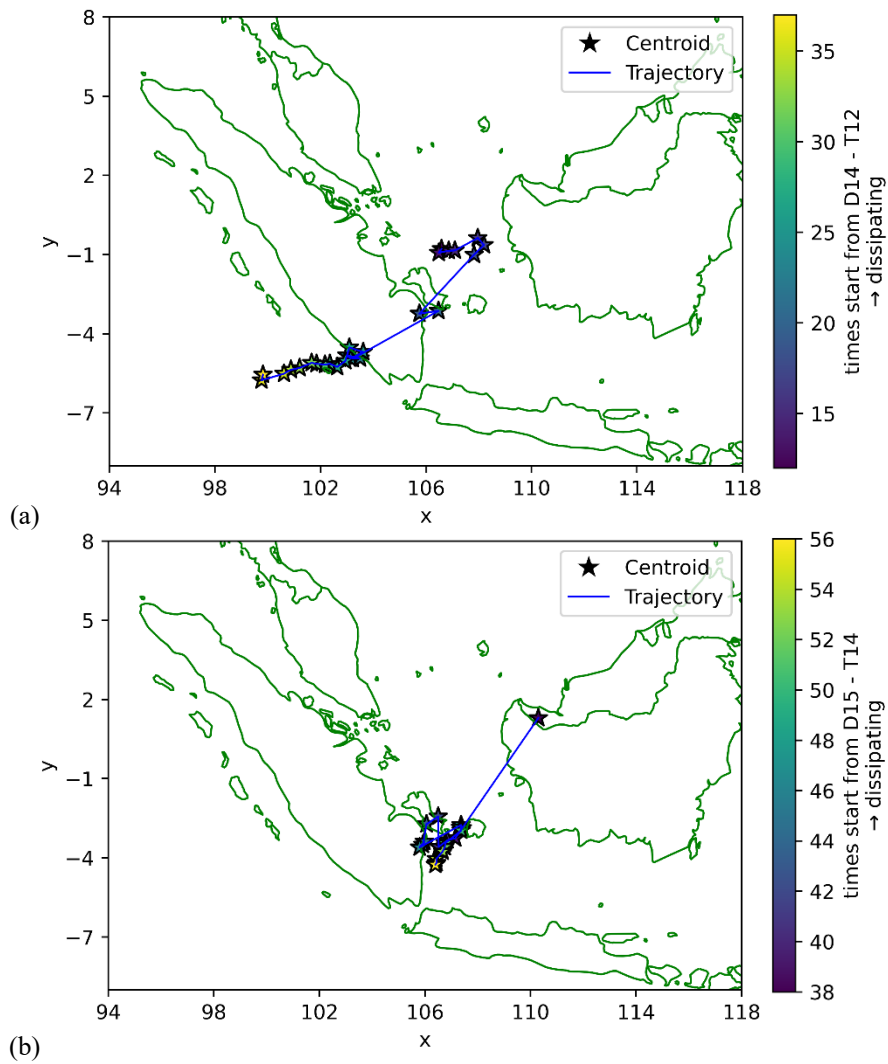
75

Figure 7. (a). same as Figure 6(a), but for the second case on July 15, 14:00 (left) and (right). (b). same as (a), but for 15:00 (left) and (right). (c). same as (a), but for 17:00 (left) and (right).
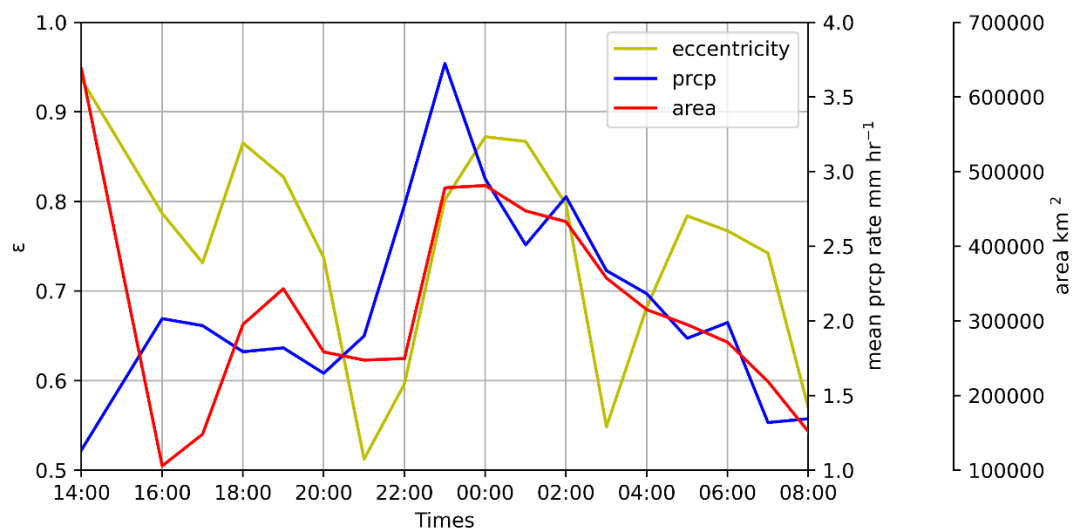
The entire boundary generated by TAMS through black body temperature data is well proved by displaying a spatial map of precipitation from GSMaP. All images depict high precipitation intensity in the cold core area of clouds with temperatures <219 K. Both CCSs in the second case continue to propagate the system and dissipate for south CCC on July 16, 08:00. Based on Figure 8, a CCC filter was performed to simulate the CCC propagating towards Belitung. This process entailed filtering the system classification with the same parents. The centroid was generated from the midpoint of the boundary area of the CCC. This analysis did not consider the CCC data that propagated northward, as the objective was to examine the CCC impact on the flood event in east Belitung. The wind confirms the southward propagation direction streamline in Figure 5(a), which shows a cyclonic circulation in southwest Sumatra.
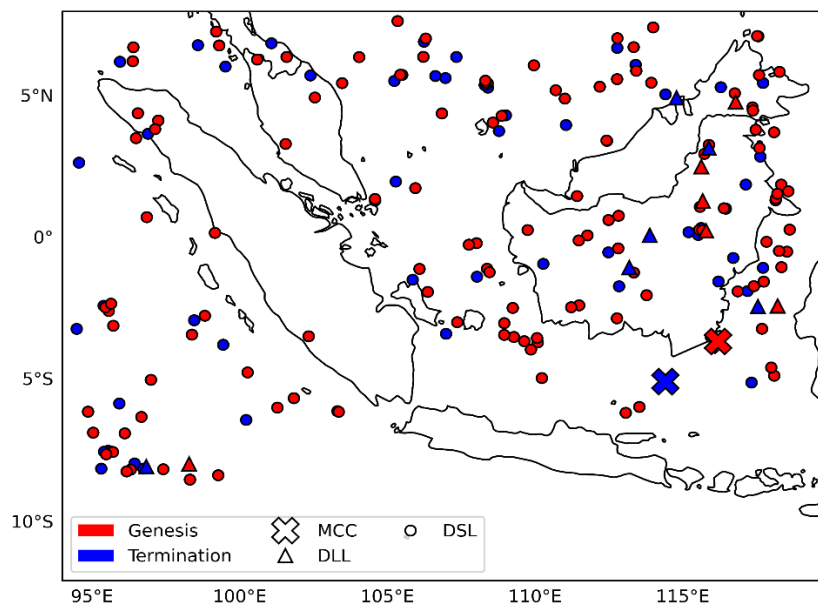
Figure 8. (a). filtered centroid and trajectory CCC for the first case, darker and shine shade indicates the initial stage and dissipating stage, respectively, D14 – T12 stated as day 14 time 12:00. (b). same as (a), but for the second case.

Figure 9. Second case variable comparison, y-axis (left) for eccentricity, y-axis (right) mean precipitation over the region of CEs area (mm hr^{-1}), and twin-y-axis (right) for the area (km^2) of MCSs.

IMPLEMENTATION OF TRACKING ALGORITHM...Sanaullah Zehri, et al.

77

Figure 10. Centroid of genesis and terminate for MCSs type except for CCC through July 14 – 16, 2017.

This may be the reason why the propagation direction of the CCC shifted southward. However, it's important to note that the flooding event was not caused by the direction of propagation but by the formation of CCC over the Belitung area. Confirming the previous research, we also assign the precipitation data, and Figure 9 shows the time evolution of eccentricity, mean precipitation, and area for clouds. It indicates that the shape of clouds becomes more elongated, covers a wider area, and reaches its peak precipitation over the area at 23:00. On the dissipating stage, at 08:00, the precipitation decreases, and the clouds become more circular, indicating the dissipating anvil.

Therefore, the implementation of cloud and assigning precipitation data into this algorithmic model has the effect of providing a more symmetrical representation of the process involved in the formation and dissipation of a storm system. The genesis and termination of all MCS types except for CCC are depicted in Figure 10. There is no particular pattern of MCS distribution in the western area, which means that due to local influences, convective activity could happen. Indonesia Maritime Continent (IMC) is surrounded by a warm pool and has significant convective activity. In this period, Mesoscale Convective Complexes (MCC) events occurred around southern Kalimantan and terminated in the Java Sea.

4. Conclusion

We investigated the MCSs linked with persistent heavy rainfall in the eastern Belitung region during the lifetime of July 14 – 16, 2017. The implementation of the TAMS successfully detected the type of MCSs associated with persistent heavy rainfall events, namely CCC. There are two cases of CCC events from July 14 – 16, at 12:00 – 08:00. The CCC experienced decoupling from the initiation system in both cases, which caused the CCC to become two, having northward and southward propagation directions. The CCC that propagated southwards to the southern part of Sumatra (first case) and southwest of east Belitung (second case) was responsible for the persistent heavy rainfall event. In implementing the algorithm, rain has the peak value at cloud temperature met <219 K or cold core areas. The average rainfall calculated over the CCC classification boundary area has symmetrical values with convective system properties such as eccentricity and area. Rainfall reaching peak values followed by an expanding CCC area and an elongated shape, and vice versa. The atmospheric conditions with the presence of meso-low pressure around western Kalimantan caused the wind to circulate in an anticyclonic and the humidity to become high. The moisture transport value is relatively high around Bangka Belitung and the north Java Sea. The warm sea surface temperature (SST) of >29° C helps increase the updraft and fuel the CCC to live longer.

We confirmed that its not only the MCC that produces heavy rainfall. However, cloud clusters such as the CCC that formed in east Belitung can produce heavy, extreme rainfall and have an impact on flood events. Therefore, we recommend the government continue monitoring the land by improving drainage systems, reclaiming former mining excavations, and limiting land conversion. For atmospheric system monitoring, its expected that the government can provide decision support system products related to MCS types over Indonesia by then anticipating extreme rainfall events that have an impact on hydrometeorological disaster events.

For the following studies, we would like to test new assigning variables to TAMS, such as outgoing longwave radiation (OLR), classifying the possible candidate of the convective system, and simulating the convective system propagation for Seroja cyclogenesis. We would like to test and improve this algorithm for aviation activity, such as aircraft flight safety, by providing predictions of MCS propagation that could potentially disrupt flights. Therefore, we also try to innovate in establishing a decision support system product using TAMS to automatically detect and classify MCSs and predict the propagation of MCSs.

Acknowledgment

References

[1] C. S. Ramage, "ROLE O F A TROPICAL ' MARITIME CONTINENT ' IN T," no. June, pp. 365–370, 1968.

[2] J. H. Qian, "Why precipitation is mostly concentrated over islands in the maritime continent," J. Atmos. Sci., vol. 65, no. 4, pp. 1428–1441, 2008, doi: 10.1175/2007JAS2422.1.

[3] V. Moron, A. W. Robertson, J. H. Qian, and M. Ghil, "Weather types across the Maritime Continent: From the diurnal cycle to interannual variations," Front. Environ. Sci., vol. 2, no. JAN, pp. 1–19, 2015, doi: 10.3389/fenvs.2014.00065.

[4] H. Satyawardhana and E. Yulihastin, "Interaksi El Nino, Monsun, dan Topografi Lokal Terhadap Anomali Hujan di Pulau Jawa," Pus. Sains dan Teknol. Atmos., no. January, pp. 60–74, 2016, [Online]. Available: https://www.researchgate.net/publication/3092 42925

[5] B. LATOS et al., "Equatorial waves triggering extreme rainfall and floods in southwest sulawesi, indonesia," Mon. Weather Rev., vol. 149, no. 5, pp. 1381–1401, 2021, doi: 10.1175/MWR-D-20-0262.1.

[6] BNPB, "Bencana Banjir di Indonesia," 2014. https://bnpb.go.id/berita/banjir (accessed Feb. 17, 2024).

[7] S. Muis, B. Güneralp, B. Jongman, J. C. J. H. Aerts, and P. J. Ward, "Flood risk and adaptation strategies under climate change and urban expansion: A probabilistic analysis using global data.," Sci. Total Environ., vol. 538, pp. 445–457, Dec. 2015, doi: 10.1016/j.scitotenv.2015.08.068.

[8] BNPB, "Banjir Mengepung Beberapa Wilayah di Belitung dan Belitung Timur, Akses Jalan Putus," 2017. https://bnpb.go.id/berita/banjir-mengepung-beberapa-wilayah-di-belitung-dan-belitung-timur-akses-jalan-putus (accessed Feb. 17, 2024).

[9] R. ANNISYA and Y. Ishak, "KAJIAN DIMENSI SALURAN 'KOLONG' PADA KAWASAN DESA MEMPAYAK KECAMATAN DAMAR KABUPATEN BELITUNG TIMUR." Universitas Bina Darma, 2019.

[10] F. Sabri, T. Aulia, and M. Tresnanda, "Analisis banjir belitung timur," Jurna penanggulangan bencana. Diakses pada Hari Jum'at 1 Maret 2019. Pukul 1035 WIB, pp. 3–8, 2017.

[11] R. Agustira, "EVALUASI PROGRAM DRAINASE DALAM MITIGASI BENCANA BANJIR DI KABUPATEN BELITUNG TIMUR PROVINSI KEPULAUAN BANGKA BELITUNG." IPDN, 2023.

[12] J. M. Fritsch, R. J. Kane, and C. R. Chelius, "The Contribution of Mesoscale Convective Weather Systems to the Warm-Season Precipitation in the United States," 1986. [Online]. Available: https://api.semanticscholar.org/CorpusID:1234 78195

[13] I. L. Jirak, W. Cotton, and R. L. McAnelly, "Satellite and Radar Survey of Mesoscale Convective System Development," Mon. Weather Rev., vol. 131, pp. 2428–2449, 2003, [Online]. Available: https://api.semanticscholar.org/CorpusID:1875 7564

[14] W. R. Cotton, G. Bryan, and S. C. van den Heever, "Mesoscale Convective Systems," Int. Geophys., vol. 99, no. C, pp. 455–526, 2011, doi: 10.1016/S0074-6142(10)09915-8.

[15] S. Samanta, P. Murugavel, D. Gurnule, Y. J. Rao, J. Vivekanandan, and T. V. Prabha, "The Life Cycle of a Stationary Cloud Cluster during the Indian Summer Monsoon: A Microphysical Investigation Using Polarimetric C-Band Radar," Mon. Weather Rev., vol. 149, no. 11, pp. 3761–3780, 2021, doi: 10.1175/MWR-D-20-0274.1.

[16] J. L. Evans and F. A. Jaskiewicz, "Satellite-based monitoring of intraseasonal variations in tropical Pacific and Atlantic convection," Geophys. Res. Lett., vol. 28, no. 8, pp. 1511–1514, 2001, doi: 10.1029/1999GL011259.

IMPLEMENTATION OF TRACKING ALGORITHM..Sanaullah Zehri, et al.

79

[17] D. E. Nuryanto, H. Pawitan, R. Hidayat, and E. Aldrian, "Characteristics of two mesoscale convective systems (MCSs) over the Greater Jakarta: case of heavy rainfall period 15–18 January 2013," Geosci. Lett., vol. 6, no. 1, 2019, doi: 10.1186/s40562-019-0131-5.

[18] E. Yulihastin, D. E. Nuryanto, Trismidianto, and R. Muharsyah, "Improvement of heavy rainfall simulated with sst adjustment associated with mesoscale convective complexes related to severe flash flood in luwu, sulawesi, indonesia," Atmosphere (Basel)., vol. 12, no. 11, 2021, doi: 10.3390/atmos12111445.

[19] K. Whitehall et al., "Exploring a graph theory based algorithm for automated identification and characterization of large mesoscale convective systems in satellite datasets," Earth Sci. Informatics, vol. 8, no. 3, pp. 663–675, 2015, doi: 10.1007/s12145-014-0181-3.

[20] N. S. Putri, T. Hayasaka, and K. D. Whitehall, "The properties of mesoscale convective systems in Indonesia detected using the grab 'em tag 'em graph 'em (GTG) algorithm," J. Meteorol. Soc. Japan, vol. 95, no. 6, pp. 391–409, 2017, doi: 10.2151/jmsj.2017-026.

[21] D. E. Nuryanto, E. Aldrian, H. Pawitan, and R. Hidayat, "Application of graph-theory based algorithm for identifying convective complex systems over greater Jakarta basins," in IOP Conference Series: Earth and Environmental Science, IOP Publishing, 2017, p. 12002.

[22] K. M. Núñez Ocasio and Z. L. Moon, "TAMS: a tracking, classifying, and variable-assigning algorithm for mesoscale convective systems in simulated and satellite-derived datasets," Geosci. Model Dev., vol. 17, no. 15, pp. 6035–6049, 2024, doi: 10.5194/gmd-17-6035-2024.

[23] K. M. N. Ocasio, J. L. Evans, and G. S. Young, "Tracking mesoscale convective systems that are potential candidates for tropical cyclogenesis," Mon. Weather Rev., vol. 148, no. 2, pp. 655–669, 2020, doi: 10.1175/MWR-D-19-0070.1.

[24] N. Nishi, A. Hamada, and H. Hirose, "Improvement of Cirrus Cloud-Top height estimation using geostationary satellite split-window measurements trained with CALIPSO data," Sci. Online Lett. Atmos., vol. 13, pp. 240–245, 2017, doi: 10.2151/sola.2017-044.

[25] T. Kubota et al., "Global Satellite Mapping of Precipitation (GSMaP) Products in the GPM Era," in Satellite Precipitation Measurement: Volume 1, V. Levizzani, C. Kidd, D. B. Kirschbaum, C. D. Kummerow, K. Nakamura, and F. J. Turk, Eds., Cham: Springer International Publishing, 2020, pp. 355–373. doi: 10.1007/978-3-030-24568-9_20.

[26] R. A. Maddox and M. C. Complexes, "Mesoscale Convective Complexes Published by : American Meteorological Society locus on forasliog," vol. 61, no. 11, pp. 1374–1387, 1980.

[27] B. E. Mapes and R. A. Houze, "Cloud clusters and superclusters over the oceanic warm pool," Mon. Weather Rev., vol. 121, pp. 1398–1415, 1993, [Online]. Available: https://api.semanticscholar.org/CorpusID:129573130

[28] V. Mathon and H. Laurent, "Life cycle of Sahelian mesoscale convective cloud systems," Q. J. R. Meteorol. Soc., vol. 127, no. 572, pp. 377–406, 2001, doi: 10.1002/qj.49712757208.

[29] G. Tsakraklides and J. L. Evans, "Global and Regional Diurnal Variations of Organized Convection," J. Clim., vol. 16, no. 10, pp. 1562–1572, Oct. 2003, [Online]. Available: http://www.jstor.org/stable/26249720

[30] S. Good et al., "The current configuration of the OSTIA system for operational production of foundation sea surface temperature and ice concentration analyses," Remote Sens., vol. 12, no. 4, pp. 1–20, 2020, doi: 10.3390/rs12040720.

[31] N. G. Loeb et al., "Advances in Understanding Top-of-Atmosphere Radiation Variability from Satellite Observations," Surv. Geophys., vol. 33, no. 3–4, pp. 359–385, 2012, doi: 10.1007/s10712-012-9175-1.

[32] H. Hersbach et al., "The ERA5 global reanalysis," Q. J. R. Meteorol. Soc., vol. 146, no. 730, pp. 1999–2049, 2020, doi: 10.1002/qj.3803.

[33] E. Aldrian and R. Dwi Susanto, "Identification of three dominant rainfall regions within Indonesia and their relationship to sea surface temperature," Int. J. Climatol., vol. 23, no. 12, pp. 1435–1452, 2003, doi: 10.1002/joc.950.

[34] J. A. I. Paski, I. J. A. Saragih, D. S. Permana, M. I. Hastuti, A. Kristianto, and E. E. S. Makmur, "Simulation of land-sea breeze effect on the diurnal cycle of convective activity in the eastern coast of north sumatra using WRF model," AGERS 2019 - 2nd IEEE Asia-Pacific Conf. Geosci. Electron. Remote Sens. Technol. Underst. Forecast. Dyn. Land, Ocean Marit. Proceeding, pp. 67–71, 2019, doi: 10.1109/AGERS48446.2019.9034301.

[35] E. Yulihastin, T. W. Hadi, N. S. Ningsih, and M. R. Syahputra, "Early morning peaks in the diurnal cycle of precipitation over the northern coast of West Java and possible influencing factors," Ann. Geophys., vol. 38, no. 1, pp. 231–242, 2020, doi: 10.5194/angeo-38-231-2020.

[36] S. Koseki, T. Y. Koh, and C. K. Teo, "Effects of the cold tongue in the South China Sea on the monsoon, diurnal cycle and rainfall in the Maritime Continent," Q. J. R. Meteorol. Soc., vol. 139, 2013, [Online]. Available: https://api.semanticscholar.org/CorpusID:122224723

[37] S. Mori et al., "Meridional march of diurnal rainfall over Jakarta, Indonesia, observed with a C-band Doppler radar: an overview of the HARIMAU2010 campaign," Prog. Earth Planet. Sci., vol. 5, pp. 1–23, 2018.

[38] M. H. M. Anip and M. A. Hisham, "The interannual and interdecadal variability of the Borneo vortex during boreal winter monsoon," 2012. [Online]. Available: https://api.semanticscholar.org/CorpusID:13346 7830

[39] SUDIAR, "Kajian Kejadian Borneo Vortex Pada Saat Terjadi Fenomena Enso Study of Borneo Vortex Events At the Time of the Enso Phenomena Sudiar," vol. 4, no. 3, pp. 31–41, 2023, [Online]. Available: https://www.ncdc.noaa.gov/teleconnecti

[40] W. Tan, X. Wang, W. Wang, C. Wang, and J. Zuo, "Different responses of sea surface temperature in the South China Sea to various El Niño events during boreal autumn," J. Clim., vol. 29, no. 3, pp. 1127–1142, 2016, doi: 10.1175/JCLI-D-15-0338.1.

[41] E. Yulihastin et al., "Evolution of double vortices induce tropical cyclogenesis of Seroja over Flores, Indonesia," Nat. Hazards, vol. 117, no. 3, pp. 2675–2692, 2023, doi: 10.1007/s11069-023-05961-8.

[42] Kementerian Lingkungan Hidup dan Kehutanan, "Rencana Strategis Direktorat Jenderal Planologi Kehutanan dan Tata Lingkungan 2020-2024," 2017. https://pktl.menlhk.go.id/data_strategis

IMPLEMENTATION OF TRACKING ALGORITHM..Sanaullah Zehri, et al.

81